Settlement of Ring Footing Resting on Geocell Reinforced Sandy Soil under Cyclic Load

Mohammed Y. Fattah[1, a], Mohammed A. Al-Neami[1, b*], Sadan A. Mohammed[1, c]

[1]Civil Engineering Department, University of Technology-Iraq, Baghdad, Iraq.

[a]40011@uotechnology.edu.iq, [b]40008@uotechnology.edu.iq, [c]sadan.azmi@gmail.com

Abstract. Ring footings are widely used as a foundation for water tanks, television antennas, silos, chimneys, oil storage tanks, etc. This paper is conducted to study the ring footing model's experimental cyclic behavior and circular footing resting on sandy soil reinforced with geocell. A group of ninety-six test models has been tested to investigate shallow footings' behavior beneath a cyclic loading of various loading rates. Four shapes of footing sand with three relative densities, two embedment depths of footing, two loading rates, and two widths of geocell were used. It was founded that as the footing depth increases, the settlement of soil due to cyclic loading decreases. Generally, when other variables are maintained to be the same, the footing bearing capacity increases when the foundation depth increases. The footing rebounds to some degree during the decay period of the load. The presence of geocell at the footing depth equals 100 mm will provide more improvement in all footing models more than using it at the surface, especially in ring 2 where the radius ratio is 0.4.

Keywords: Reinforced sand; ring foundations; geocell reinforcement; cyclic loading.

Introduction

Soil strengthening using reinforcement is not a new science but has a long history. Henri Vidal, a French architect, and engineer was the first to use systemic soil reinforcement in modern society. Binquet and Lee [1] pioneered research with planar aluminum strips, which began the systematic research. Metal reinforcement in a planar shape, which is expensive and corrosive, was commonly used in the past. However, the discovery of polymeric geosynthetics has resulted in a soil reinforcement revolution. Geocell is the most recent trend in geosynthetic-reinforcement. Several influencing parameters have been investigated, but the information parametric effect has yet to be completely exploited. Since the 1970s, geosynthetics have been commonly used as soil reinforcement material. Generally, ring footings are usually circular and constructed to support walls or columns of axisymmetric structures. This type of foundation may use as a foundation for transmission towers, water towers, silos, television antennas, oil storage, and chimneys because the ring footings provide a more suitable and low-cost- design. Fischer [2] proposed an analytical solution to calculate the flexible ring footings' settlement depended on the elasticity and superposition principle for a semi-infinite elastic. Later,

Egorov [3] suggested several numerical relationships to predict the settlement and bearing capacity under flexible and rigid ring footings. Also, Bowles [4] used the finite element method to predict the settlement and bearing capacity of ring footings. Rajagopal et al. [5] studied the behavior of stiffness and strength of sand confined in single and multiple geocells using triaxial tests. They concluded that in granular soil and due to geocell confinement, the apparent cohesive strength increases, while the frictional strength is not affected. Hataf and Razavi, [6] found that radius ratio (n) (n is the ratio of internal radius (r_i) to an external radius (r_o)) value for the maximum bearing capacity of sand is not a unique value but is in the range of (0.2 to 0.4). Also, they proposed a semi-empirical relationship to predict the unit bearing capacity of ring footings constructed on sandy soil. Sudhakar and Sandeep [7] carried out experimental research to study the ring footing model's static and cyclic behavior and circular footing embedded in the sand reinforced with geocell. Coir geocell was adopted as a material reinforcement to strengthen the soil. The findings showed that geocells for strengthening sand

cushion reduce settlement of both ring and circle footings by a significant amount due to a change in stress distribution. The embedding geocell mattress's width and depth were found to positively impact developed bearing ability and settlement reduction. In general, many studies have been published that look at the behavior of geocell reinforced soils under static and dynamic loads. However, only a few studies have dealt with ring footings' behavior under static and cyclic load. Therefore, this study investigates the behavior of ring footings with various radius ratios resting on sandy soil reinforced with geocells materials under the cyclic load.

Laboratory Work

Soil Used. Air-dried sand used in the current study was taken from Karbala city in Iraq. The properties of the used sand include grain size distribution, specific gravity, and maximum and minimum dry densities were measured. Table 1 summarizes the testing results in accordance with standard specification had been followed for each testing. According to the Unified Soil Classification System (USCS), the sand is classified as (SP) medium to coarse, poorly graded sand.

Table 1. Physical properties of the tested sand.

Property	Value	ASTM Standard
Specific gravity (G_s)	2.675	D 854 [8]
D_{10} D_{30} D_{50} D_{60} (mm)	0.239, 0.41, 0.8, 1.38	D 422 [9] and D 2487 [10]
Coefficient of uniformity, (C_u)	5.79	
Coefficient of curvature, (C_c)	0.50	
USCS Soil classification	SP	
Maximum dry unit weight (kN/m³)	19.52	D 4253 [11]
Minimum dry unit weight (kN/m³)	16.63	D 4254 [12]
Void ratio, (e_{max})	0.6	----------
Void ratio, (e_{min})	0.37	----------
Friction angle at RD = 30, 55, and 85%	35.2°, 40.2° and 44.7°	D 3080 [13]

Geocell Reinforcement. In this study, a used geocell reinforcement was manufactured from the planar polymeric taps that were periodically sewn to the adjacent taps to create a "honeycomb" arrangement; as a result, a non-perforated flexible geocell was made locally. The geocell walls height is (50 mm), the geocell pocket size (d) is kept constant (d = 50 mm), which is taken as a diameter of an equivalent circular area of the pocket opening (Ag) (i.e., $d^2 = 4/\pi \times Ag$). The d/B ratio equal to 0.5 (i.e. d/B = 0.5) (where B is the model footing width). Also, two different geocell mat widths (b) were used (b_1= 10 cm, and b_2= 20 cm) as depicted in Figure 1. Also, the tensile modulus and strength of the used geocell were determined using the tensile test following ASTM D6637 [14]. The results showed that tensile modulus, M is 0.75 MPa, while yield strength is 39.53 MPa.

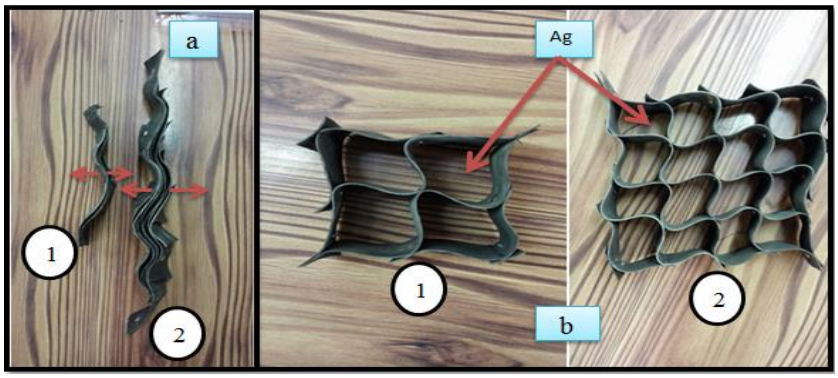

Figure 1. (a) geocell used before the expansion. (b) geocell used after the expansion.

Setup Design and Manufacturing of Loading Machine

To evaluate various variables influence in transferring of the cyclic loading due to the fluid (in water tanks) motion in the sand, it is necessary to simulate the situations as closely as possible to those that occur on-site. To satisfy this objective, a special testing apparatus and accessories were manufactured. The loading machine has the ability to apply a wide range of cyclic loads by using two pneumatic cylinders; cylinder 1 used for a low range load begins from 153.7N to 442N while cylinder 2 is used for medium to high range load, which begins from 375N to 1171.9N. Figure 2 shows the view of the manufactured apparatus and the pneumatic cylinders. The manufactured loading machine, which was manufactured by Tawfiq [15], involves the following:

1. The frame of steel loading,
2. System of axial loading,
3. Footing,
4. Testing box, and
5. The measurement device of shear strength.

Steel Frame of Loading. The steel frame was manufactured to support the pneumatic jack and to satisfy the jack's ability to apply a vertical loading on the footing model as depicted in Figure 3. The loading frame is consisting of four transverse steel beams and four steel columns. Each member of the frame is a rectangular shape of (120×65 mm) a cross-sectional area with 4 mm wall thickness. The dimensions of a frame are (1150×810×1520 mm), which represent the (length × width × height), respectively. To increase the frame supporting withstand the loads, two extra beams were welded to the frame of steel load, as shown in Figure 4. A steel plate of 25 mm thick with dimensions of (800×300 mm) was connected with the transverse beam by using four bolts (20 mm diameter) (Figure 5). The loading frame was connected to the floor base by four base plates with dimensions of (250×250×10 mm). Four anchor bolts with a diameter of 12 mm were used to fix each base plate with the floor.

Figure 2. Details description of the apparatus.
(1- loading Steel frame, 2- Vertical loading system, 3- footing model, 4- Steel box, 5- Strength measurement device, 6- Controlling system, 7- Compressor).

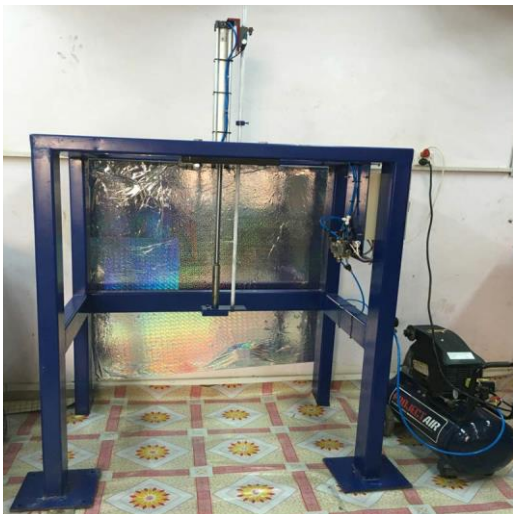

Figure 3. Frame of the steel loading.

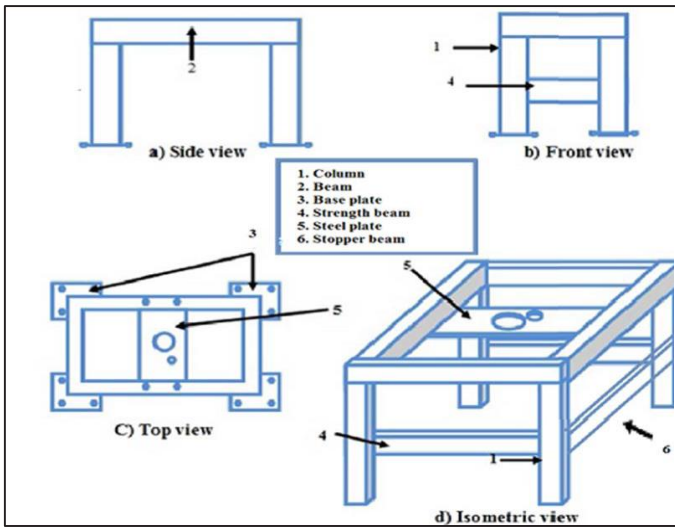

Figure 4. Loading frame schematic diagram [15].

Figure 5. Steel plate for supporting a jack.

Axial Loading System. The axial load system is consisting of:

Pneumatic cylinder. As mentioned previously, two pneumatic cylinders have formed this system; the first cylinder was used for a low range load and applied a force in between 153.72 - 442 N, (cylinder1). The second cylinder is a medium and high range load cylinder (375 to 1171.9 N), and it uses to apply a medium and high load (cylinder 2). The body of cylinders described above was made from aluminum material, while the shaft was manufactured from medium carbon steel. Nickel- chrome is used and coated the shaft to increase its smoothness and to decrease the friction effect that occurred with the packing. The piston is manufactured using aluminum, while the Viton is used in pressure washer- packing. The pneumatic valves are fixed to the two cylinders with a flexible hose. The peak pressure can be operated using the two cylinders is 100 kPa (10 bars). Both cylinders contain a piston that has an outer diameter equal to the inner diameter of each cylinder. Cylinder1has an inner diameter of 32mm while the inner diameter of cylinder2 is 50 mm. This piston's movement is similar for both cylinders, and it moves up and down with a stroke equal to 500 mm. Moreover, the first cylinder's piston is connected with a movable shaft with a 10 mm diameter, while the piston in the second cylinder is connected with another movable shaft with a 20 mm diameter. This movable shaft was threaded and connected at it one end with upper footing. It is worth noting that the shaft threads have dimensions similar to the used cylinders and the same to the upper footing model of a device used. For both cylinders and the second side of the device top (upper movable plate or upper-pressure plate) another shaft with 14 mm in diameter was installed. This shaft is used

to avoid or prevent the footing rotation (the circular or ring footing model is used in tests) during moving down and up with the cylinder movement's piston, as illustrated in Figure 6.

System of air compressor. A 40-liter metal vessel with a pressure capacity greater than 10 bar is used in the compressed air system (Project air brand). The compressed air device consists of a silicon aluminum alloy air compressor with a way valve and an air reducing valve. An electric motor drives a compressor with a 2.5 kW and 220 Voltage (single phase motor) a 50 Hz frequency, and 1450 rpm rotation speed.

Figure 6. The shaft of 14 mm in diameter.

Control system. It controls the movement of the device under the influence of loads applied, either cyclic loading or monotonic. This system consists of two directional valves, the first is for auto operation, and the other is used for the manual operation with electrical control; these valves control the movement of a pneumatic cylinder; Figure 7 shows the electrical. The electric panel is connected to the device to operate by two buttons manually; the first button is used for the upward movement while the other is used for the movement downward or automatically running through the relays and time. It is necessary to note that when a cyclic load is used, the frequency must be determined to form the desired function as a relationship between the applied force and time (in seconds). This is implemented by using a C-type unit. A mathematical form is different slightly from that of the function in practice, as illustrated in Figure 8.

Figure 7. Control system – a general view.

Footing Model and Container

To study the dimension's influence of the foundation, four steel foundations has 20 mm thickness are used, a circular footing model with (100 mm) diameter, three-ring footings (R_1, R_2, and R_3) with an inner diameter of (30, 40, and 50) mm respectively and outer diameter for

all is kept equals (100 mm). The soil box used in this study is a square made as a one-piece steel plate that has a (6 mm) thickness with a cross-section of (700×700) mm with a depth of 800 mm.

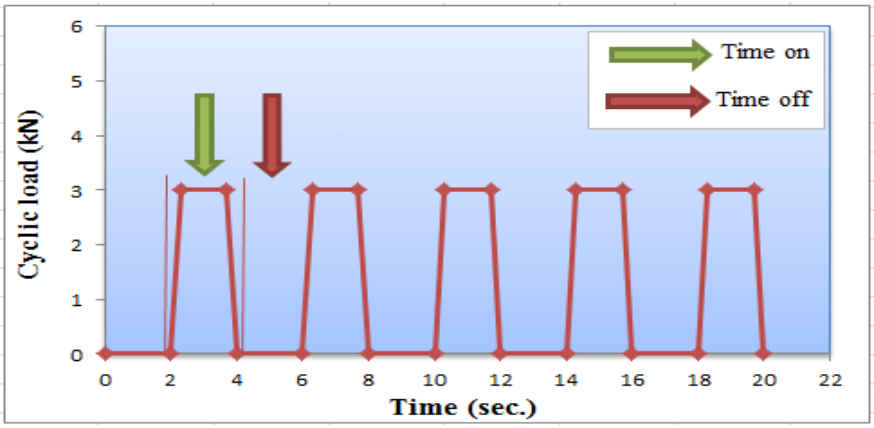

Figure 8. Realistic load-time relationship.

Instrumentation

LVDT was used to record the footing settlement during testing under the applied cyclic load. LVDT used in this study has a 50 mm stroke with a range of ±10 V output signal and normal DC power supply equals 10 V. The measuring of settlement is made at a footing surface "from the edge". To ensure a good connection in between the upper surface of footing and LVDT, a special technique was adopted. Data acquisition was used to automatically scan and record the data using the data logger and computer (Figure 9). The load cell (compression/tension) was connected with a digital weighing indicator to display and record applied load value.

Figure 9. Linear variable differential transformer (LVDT).

Model Test Results under Cyclic Load

A total of 96 test models was carried out on dry sandy soil beneath cyclic loading, 48 of these models are conducted with the geocell reinforcement of constant placement depth (u) as (0.3B), and geocell width (b) is selected as B & 2B (where B is the footing width and equals 100 mm for all foundations). These adopted values were recommended by Dash et al. [16], who stated that the optimum depth of geocell placement (u) after normalized with a width of footing (B) or diameter of footing (D) is 0.1 – < 0.33 D (or B) from the bottom of the footing. Another

48 models were tested without geocell reinforcement using various relative densities of sand; 30%, 55%, and 85%, which represent respectively "loose sand, medium sand, and dense sand". For all test models, the failure criterion is determined according to Terzaghi [17]. To choose the applied load magnitude on the footing, the footing's theoretical ultimate bearing capacity was calculated according to the parameters; friction angle, relative density, foundation shape, foundation depth, and foundation width (or diameter). The theoretical calculations were made, according to Hansen equation [18]:

$$q_{ult} = c\,N_c S_c d_c i_c g_c b_c + q\,N_q\,S_q\,d_q\,i_q\,g_q b_q + 0.5\,\gamma\,B\,N_\gamma\,S_\gamma d_\gamma\,i_\gamma\,g_\gamma\,b_\gamma \quad (1)$$

Where q_{ult} is the ultimate bearing capacity (kPa), c is the soil cohesion (kPa), q is the surcharge ($\gamma\,\boldsymbol{D_f}$) (kPa), D_f is the footing depth (m), Nc, Nq, and Nγ are factors of the bearing capacity due to soil cohesion, surcharge stress and unit weight of respectively, B is the foundation diameter (m), γ is the soil unit weight (kN/m^3), S_c, S_q, S_γ are factors of the shape, d_c, d_q, d_γ are factors of the depth, i_c, i_q, i_γ are factors of the inclination, g_c, g_q, g_γ = are factors of the ground, and b_c, b_q, b_γ are factors of the base. The allowable load in the case of reinforced soil is obtained by multiplying the unreinforced allowable load by improvement factor (IF), which is equal to 1.85; this value was taken compatible with the findings of Moghaddas Tafreshi and Dawson [19]:

$$IF = \frac{q_{geocell}}{q_{unrein}} \quad (2)$$

Where q_{unrein} is the bearing pressure of the unreinforced soil (kPa), $q_{geocell}$ is the bearing pressure of the geocell reinforced soil (kPa), and IF is the improvement factor in bearing pressure of footing due to geocell reinforcement. Because the soil used is sand and the footing put at the soil surface, the values of c and Dr are excluded, so Equation 1 becomes:

$$q_{ult} = 0.5\,\gamma\,B\,N_\gamma\,S_\gamma\,d_\gamma\,i_\gamma\,g_\gamma b_\gamma \quad (3)$$

In this study, $i_\gamma, g_\gamma, b_\gamma$ are equal to 1, so Equation 1 becomes:

$$q_{ult} = 0.5\,\gamma\,B\,N_\gamma\,S_\gamma d_\gamma \quad (4)$$

In this study, B = 100 mm, and if D_f =B = 100 mm, so Equation 1 becomes:

$$q_{ult} = qN_qS_qd_q + 0.5\gamma BN_\gamma S_\gamma d_\gamma \quad (5)$$

Tables 2 and 3 present the outcomes of q_{ult}, q_{all}; and friction angle founded by the direct shear test in addition to the applied load, in experiments for both unreinforced and reinforced models, the safety factor is equal to (1.5). It is noticed that only when the footing is $ring_1$, $ring_2$ and $ring_3$, D_f = 0 and sand density=30%, the applied loading; through tests will be greater than the footing Q_{all} for both cases unreinforced and reinforced, since the minimum applied load that can project by the device is approximately (154 N), i.e., (F.S.< 1.5). Also, it can be seen that the values of the internal friction angle (ϕ) in reinforced soil is considered the same as unreinforced soil, since the direct shear test available in the laboratory was with small shear box dimensions, and it is not enough for placing both the soil and geocell in it. Therefore large-scale shear box size is required for testing reinforced sand. In general, if the sand is tested with reinforcement, its strength will be almost higher than the unreinforced one, according to what has been mentioned in the literature reviews. The assumption of considering the same value of (ϕ) for unreinforced and reinforced models was validated by Rajagopal et al. [5], who concluded that confinement of geocell had no effect on the frictional strength of the granular soil.

Table 2. Theoretical values of the calculated static bearing capacity (unreinforced models).

Foundation Type	Soil State	φ (°)	γ (kN/m^3)	D_f mm	Theoretical $q_{ult.}$ (kPa)	Theoretical $Q_{all.}$ (N)	Applied Load (N)
Circular, D=100 mm	Loose	35.2	16.8	0	17.88	160	154
				100	131.94	690.84	154
	Medium	40.2	17.52	0	44.28	231	192
				100	278.03	1455.76	192
	Dense	44.7	18.48	0	107.13	560.93	231
				100	589.14	3084.73	231
$Ring_1$, D_{in}/D_{out}=0.3	Loose	35.2	16.8	0	17.88	150	154
				100	131.94	628.66	154
	Medium	40.2	17.52	0	44.28	210.98	192
				100	278.03	1324.74	192
	Dense	44.7	18.48	0	107.13	510.45	231
				100	589.14	2807.1	231
$Ring_2$ D_{in}/D_{out}=0.4	Loose	35.2	16.8	0	17.88	140	154
				100	131.94	580.3	154
	Medium	40.2	17.52	0	44.28	194.75	192
				100	278.03	1222.84	192
	Dense	44.7	18.48	0	107.13	471.18	231
				100	589.14	2591.17	231
$Ring_3$, D_{in}/D_{out}=0.5	Loose	35.2	16.8	0	17.88	130	154
				100	131.94	518.13	154
	Medium	40.2	17.52	0	44.28	173.89	192
				100	278.03	1091.82	192
	Dense	44.7	18.48	0	107.13	420.7	231
				100	589.14	2313.55	231

Table 3: Theoretical values of the calculated static bearing capacity (Reinforced models).

Foundation Type	Soil State	φ (°)	γ (kN/m^3)	D_f (mm)	Theoretical $q_{ult.}$ (kPa)	Theoretical $Q_{all.}$ (N)	Applied Load (N)
Circular, D=100 mm	Loose	35.2	16.8	0	33.08	296	375
				100	244.09	1278.05	375
	Medium	40.2	17.52	0	81.92	427.35	469
				100	514.36	2693.16	469
	Dense	44.7	18.48	0	198.2	1037.72	563
				100	1090	5706.75	563
$Ring_1$, D_{in}/D_{out}=0.3	Loose	35.2	16.8	0	33.08	277.5	375
				100	244.09	1163.02	375
	Medium	40.2	17.52	0	81.92	390.31	469
				100	514.36	2450.77	469
	Dense	44.7	18.48	0	198.2	944.33	563
				100	1090	5193.14	563
$Ring_2$, D_{in}/D_{out}=0.4	Loose	35.2	16.8	0	33.08	259	375
				100	244.09	1073.56	375
	Medium	40.2	17.52	0	81.92	360.29	469

				100	514.36	2262.25	469
	Dense	44.7	18.48	0	198.2	871.68	563
				100	1090	4793.66	563
$Ring_{3,}$ D_{in}/D_{out}=0.5	Loose	35.2	16.8	0	33.08	240.5	375
				100	244.09	958.54	375
	Medium	40.2	17.52	0	81.92	321.7	469
				100	514.36	2019.87	469
	Dense	44.7	18.48	0	198.2	778.3	563
				100	1090	4280.07	563

Effect of the depth of foundation. The footing depth is a significant variable that administers the soil ultimate bearing capacity. Generally, when the applied cyclic loading on a footing is less than Q_{all}, the other parameters such as R.D., footing shape, the width of geocell, total time of load, and loading rate were retained constant, but the foundation depth is only different. Two foundation depths were used:

- At the soil surface,
- At depth 100 mm (B).

From Figures 10, 11 and 12 in general for both unreinforced and reinforced models, it can be observed that as the footing depth (D_f) increases, the settlement of the soil decreased and after the test, the angle of internal friction (ϕ) increases comparing with surface state of the same other parameters, as a result, to increase in the surcharge weight, and this causes an increase in the bearing capacity of the soil. These results are compatible with Dixit and Patil's findings [20], who concluded that, generally, when other variables are kept constant, the bearing capacity of soil goes on rising when the depth of foundation increases. In addition, Fattah et al. [21] found that when the cyclic applied load on a footing is less than Q_{all}, other variables such as system velocity (loading rate), the relative density of sand, footing type, and total time remained constant, but the footing depth is only varied, the settlement of soil decreased, and the bearing capacity increased.

From these results also, it can be noticed that in Figure 10 at D_f = 0, the maximum settlement value is less at ring1 and ring2 which is equal to (1.06 mm), higher in a circular (1.52 mm), and much higher in ring3 footing (1.8 mm), while in Figure 11. At D_f= 0, the maximum settlement value is less at ring 1, which is equal to (1.34 mm), less high in ring2 (1.58 mm), higher in ring3 (1.74 mm), and much higher in circular footing (2.2 mm). In Figure 10 at D_f = 100 mm, the maximum settlement value is less at ring1 which is equal to (0.47 mm), less high in a circular (0.78 mm), higher in ring 2 (0.83 mm), and much higher in ring3 footing (0.96 mm), while in Figure 11 at D_f= 100 mm, the maximum settlement value is less at ring1 which is equal to (0.5 mm), higher in ring 3 (0.95 mm) and much higher in circular and ring 2 footings (1.3 mm), so these values show that in general, the maximum settlement value is less in ring1 and much higher in ring 3.

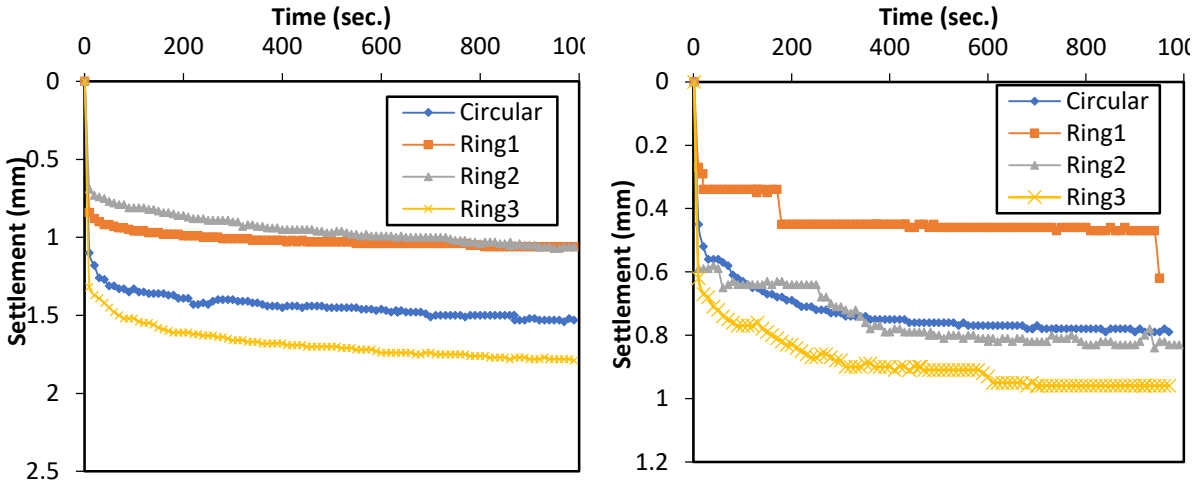

a) at surface, Df = 0. b) at depth B, Df =100 mm.

Figure 10. Settlement change with time at R.D. = 30% and velocity= 5 mm/sec at different depths of footing (Unreinforced sand).

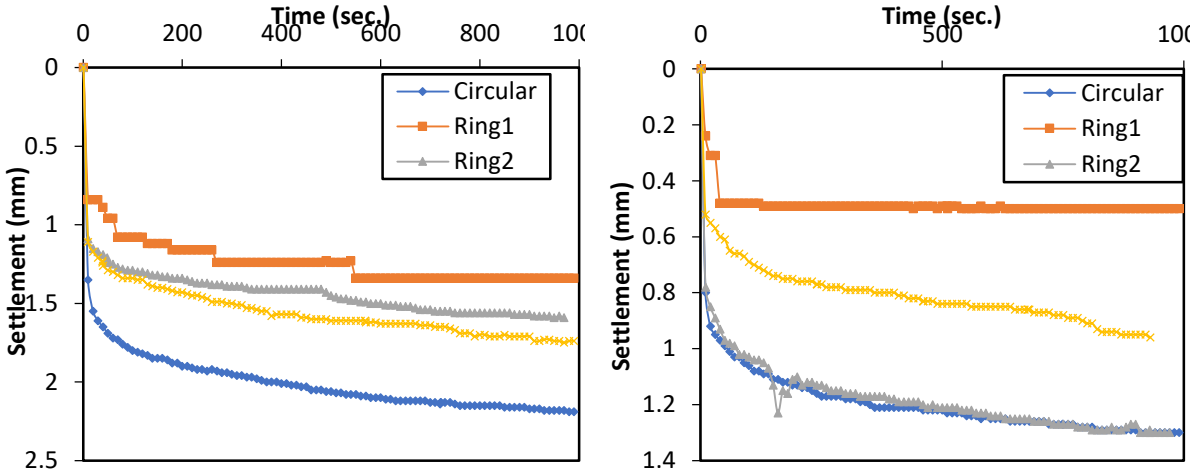

a) at surface, Df = 0. b) at depth B, Df =100 mm.

Figure 11. Settlement change with time at R.D. = 55% and velocity= 5 mm/sec at different depths of footing (Unreinforced sand).

From Figure 12, it can be noticed that the geocell with width (b1=100 mm) at depth D_f = 100 mm provided an improvement in all four footings more than using it at the surface, especially in ring 2, the settlement decreased to half and in-ring 3 the settlement decreased to the quarter. It can be noticed that most of the displacement response of footings occur in the first few cycles then with the number of cycles, the rate of footing settlement decreased significantly [19, 22].

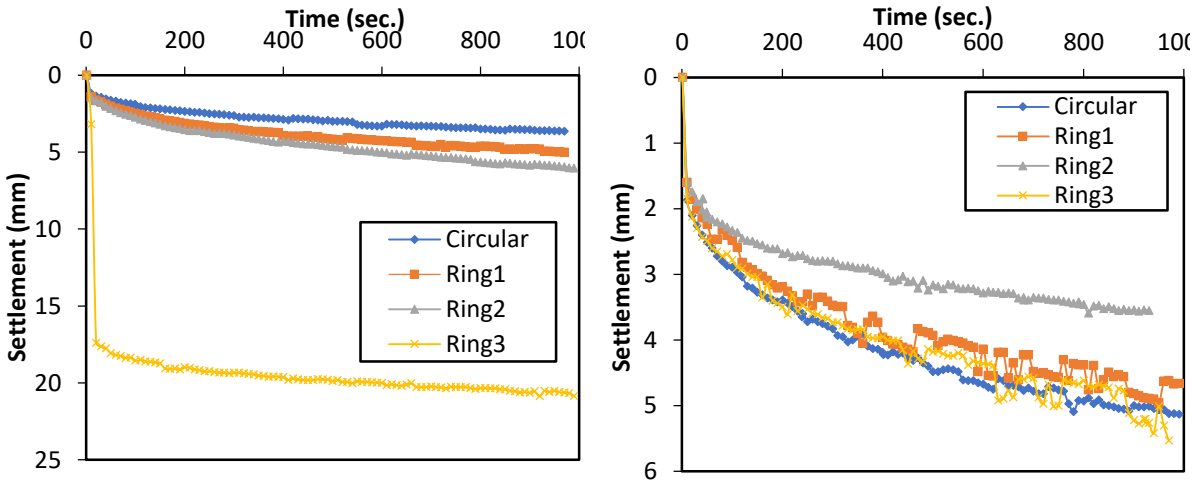

a) at surface, Df = 0. b) at depth B, Df =100 mm.

Figure 12. Settlement change with time at R.D. = 85%, b1=100 mm and velocity= 5 mm/sec. at different depths of footing (Reinforced sand).

It is worth mentioning that the settlement recorded for reinforced models is greater than that for unreinforced models because the reinforced models were subjected to higher loads. Despite that, the recorded settlement was small and lower than an allowable settlement for shallow footings. Generally, the presence of geocell offers lateral restraint that prevents the sand from spreading and hence reduces the stress coming onto the underlying soil. The reinforced models' settlement is greater than that for unreinforced models because the reinforced models were subjected to higher loads. Despite that, the recorded settlements were small and lower than allowable settlement for shallow footings.

Conclusions

- For both unreinforced and reinforced models, as (Df) the footing depth increases, the settlement of soil due to cyclic loading decreases. Generally, when other variables are maintained to be the same, the footing bearing capacity goes on increasing when the foundation depth increases.
- Generally, the maximum settlement value is less in ring1 and much higher in ring3 in different depths of footing in the case of unreinforced models. The presence of geocell at Df =100 mm will improve all footing models more than using it at the surface, especially in ring2.
- Ring 2 with (Din/Dout= 0.4) is the closest one to the circular footing with the same outer diameter. In the case of cyclic loading, in each phase, and due to unloading, a small amount of settlement is rebounded, and this is considered to be either recoverable or elastic settlement, while a great portion of the settlement is a plastic settlement and kept in the system. This enables the designers to use ring 2 as an alternative to the circular footing, which leads to a benefit in reducing the construction cost.

References

[1] Binquet, J. and Lee, K.L., 1975. Bearing capacity tests on reinforced earth slabs. Journal of the geotechnical Engineering Division, 101(12), pp.1241-1255.

[2] Fischer, K., 1957. Zur Berechnungdersetzung Von undamenten in derformeiner Kreisformigen Ring flache. Der Bauingenieur, 32, 172–174 (in German).

[3] Egorov, K.E., 1965. Calculation of bed for foundation with ring footing. Proceedings of the Sixth International Conference on Soil Mechanical Foundation of Engineers, 2, 41–45.
[4] Bowles, J.E. 1977. Foundation analysis and design. 5th Edition. McGraw-Hill.
[5] Rajagopal, K., Krishnaswamy, N.R. and Latha, G.M., 1999. Behaviour of sand confined with single and multiple geocells. Geotextiles and Geomembranes, 17(3), pp.171-184.
[6] Hataf, N., and Razavi, M.R., 2003. Behavior of ring footing on sand. Iranian Journal of Science and Technology, Transaction B, 27, 47–56.
[7] Sudhakar, A.R. and Sandeep, M.N., 2016. Incremental cyclic loading on ring and circular footing resting on geocell reinforced sandy soil. International Journal of Advance Research, 3, pp.52-56.
[8] American Society of Testing and Materials, ASTM, 2006. Standard test method for specific gravity of soil solids by water pycnometer" ASTM D854, West Conshohocken, Pennsylvania, USA.
[9] American Society of Testing and Materials, ASTM., 2006. Standard test method for particle size-analysis of soils. ASTM D422-02, West Conshohocken, Pennsylvania, USA.
[10] American Society of Testing and Materials, ASTM., 2006. Standard test method for classification of soils for engineering purposes (Unified Soil Classification System). ASTM D2487-06, West Conshohocken, Pennsylvania, USA.
[11] American Society of Testing and Materials, ASTM., 2006. Standard test method for maximum index density and unit weight of soils using a vibratory table. ASTM D4253-06, West Conshohocken, Pennsylvania, USA.
[12] American Society of Testing and Materials, ASTM., 2006. Standard test method for minimum index density and unit weight of soils and calculation of relative density. ASTM D4254-06, West Conshohocken, Pennsylvania, USA.
[13] American Society of Testing and Materials, ASTM., 2006. Standard test method for direct shear test of soils under consolidated drained conditions. ASTM D3080-06, West Conshohocken, Pennsylvania, USA.
[14] American Society of Testing and Materials, ASTM., 2008. Standard test method for determining tensile properties of geogrids by the single or multi-rib tensile method. ASTM D6637, West Conshohocken, Pennsylvania, USA.
[15] Tawfiq, H.H., 2017. Effect of uncertainties of sandy soil shear strength parameters on the reliability of foundations under cyclic loading. M.Sc. Thesis, Building and Construction Engineering Department, University of Technology, Iraq.
[16] Dash, S.K., Biswas, A., and Krishna, A.M., 2012. Parameters influencing the performance of geocell- reinforced foundation system—proceedings of Indian Geotechnical Conference, Delhi.
[17] Terzaghi, K., 1943. Theoretical Soil Mechanic, John Wiley and Sons, New York.
[18] Hansen, J.B., 1970. A revised and extended formula for bearing capacity.Bulletin of Danish Geotechnical Institutes, 28, 5–11.
[19] Tafreshi, S.M. and Dawson, A.R., 2010. Comparison of bearing capacity of a strip footing on sand with geocell and with planar forms of geotextile reinforcement. Geotextiles and Geomembranes, 28(1), pp.72-84.
[20] Dixit, M.S. and Patil, K.A., 2010. Study of effect of different parameters on bearing capacity of soil. Indian Geotechnical Society, GEOTID, pp.431-005.
[21] Fattah, M.Y., Karim, H.H. and Al-Qazzaz, H.H., 2017. Cyclic behavior of footings on dry sand under different rates of loading. International Journal of Construction Engineering and Management, 6(6), pp.240-253.
[22] Asakereh, A., Ghazavi, M. and Tafreshi, S.M., 2013. Cyclic response of footing on geogrid-reinforced sand with void. Soils and foundations, 53(3), pp.363-374.